EBioMedicine 25 (2017) 95–105

Contents lists available at ScienceDirect

EBioMedicine

journal homepage: www.ebiomedicine.com

Research Paper

American Strain of Zika Virus Causes More Severe Microcephaly Than an Old Asian Strain in Neonatal Mice

Feng Zhang [a,c,1], Hong-Jiang Wang [b,1], Qin Wang [a,c,1], Zhong-Yu Liu [b,1], Ling Yuan [a,c,1], Xing-Yao Huang [b,1], Guanghui Li [a,b], Qing Ye [b], Haozhen Yang [d], Lei Shi [a], Yong-Qiang Deng [b], Cheng-Feng Qin [b,f,*], Zhiheng Xu [a,c,e,**]

[a] State Key Laboratory of Molecular Developmental Biology, CAS Center for Excellence in Brain Science and Intelligence Technology, Institute of Genetics and Developmental Biology, Chinese Academy of Sciences, Beijing 100101, China
[b] Department of Virology, State Key Laboratory of Pathogen and Biosecurity, Beijing Institute of Microbiology and Epidemiology, Beijing, China
[c] University of Chinese Academy of Sciences, Beijing 10101, China
[d] Liver Failure Therapy and Research Center, Beijing, 302 Hospital, Beijing, China
[e] Parkinson's Disease Center, Beijing Institute for Brain Disorders, Beijing, China
[f] Guangzhou Eighth People's Hospital, Guangzhou Medical University, Guangzhou 510060, China

ARTICLE INFO

Article history:
Received 15 July 2017
Received in revised form 16 October 2017
Accepted 19 October 2017
Available online 20 October 2017

Keywords:
Zika virus
American strain
Asian strain
Microcephaly

ABSTRACT

Zika virus (ZIKV) has evolved from an overlooked mosquito-borne flavivirus into a global health threat due to its astonishing causal link to microcephaly and other disorders. ZIKV has been shown to infect neuronal progenitor cells of the fetal mouse brain, which is comparable to the first-trimester human fetal brain, and result in microcephaly. However, whether there are different effects between the contemporary ZIKV strain and its ancestral strain in the neonatal mouse brain, which is comparable with the second-trimester human fetal brain, is unclear. Here we adopted a mouse model which enables us to study the postnatal effect of ZIKV infection. We show that even 100 pfu of ZIKV can replicate and infect neurons and oligodendrocytes in most parts of the brain. Compared with the ancestral strain from Cambodia (CAM/2010), infection of the ZIKV strain from Venezuela (VEN/2016) leads to much more severe microcephaly, accompanied by more neuronal cell death, abolishment of oligodendrocyte development, and a more dramatic immune response. The serious brain damage caused by VEN/2016 infection would be helpful to elucidate why the American strain resulted in severe neurovirulence in infants and will provide clinical guidance for the diagnosis and treatment of infection by different ZIKV strains.

1. Introduction

The World Health Organization has declared the current ZIKV epidemic a Public Health Emergency of International Concern due to the causal link between the current Zika strain and congenital brain abnormalities, especially microcephaly in the fetuses and offspring of pregnant women (Rubin et al., 2016; Parra et al., 2016). Clinical investigations and animal models have provided substantial evidence that ZIKV can infect cultured neuronal progenitor cells (NPCs) and organoids from human iPSCs, or directly target mouse, pigtail macaque or human fetal brains, cause neural cell death, and lead to fetal brain lesions and microcephaly (Li et al., 2016a; Tang et al., 2016; Wu et al., 2016; Miner et al., 2016; Garcez et al., 2016; Rasmussen et al., 2016; Adams Waldorf et al., 2016).

Several recent studies have confirmed the causal link between ZIKV infection and microcephaly in embryonic mouse models infected with ZIKV (Li et al., 2016b; Wu et al., 2016; Shao et al., 2016). Contemporary ZIKV strains are able to infect the neuronal progenitor cells of fetal brains and disrupt their development including proliferation and differentiation, trigger a strong immune response, cause neuronal cell death and microcephaly in the embryonic mouse brain (Tang et al., 2016; Li et al., 2016b; Li et al., 2016c; Wu et al., 2016; Rasmussen et al., 2016). However, ZIKV was an obscure mosquito-borne flavivirus which circulated for decades in Sub-Saharan Africa and Asia since its first isolation 60 years ago (Mlakar et al., 2016; Hayes, 2009). Retrospective evidence of microcephaly in newborn patients was retrieved only after 2013–14 in French Polynesia and later in the Americas (Duffy et al., 2009; Cao-Lormeau et al., 2014). Therefore, several critical questions remain open regarding whether different ZIKV strains have different detrimental effects on brain development, and whether the contemporary ZIKV

* Correspondence to: C.F. Qin, Department of Virology, State Key Laboratory of Pathogen and Biosecurity, Beijing Institute of Microbiology and Epidemiology, Beijing, China. ** Correspondence to: Z. Xu, State Key Laboratory of Molecular Developmental Biology, CAS Center for Excellence in Brain Science and Intelligence Technology, Institute of Genetics and Developmental Biology, Chinese Academy of Sciences, Beijing 100101, China.
E-mail addresses: qincf@bmi.ac.cn (C.-F. Qin), zhxu@genetics.ac.cn (Z. Xu).
[1] These authors contributed equally to this work.

https://doi.org/10.1016/j.ebiom.2017.10.019

strains have evolved to become more neurotropic with increased replicative capacity which then plays a role in the development of microcephaly.

The CAM/2010 strain is an old Asian strain of ZIKV isolated from a Cambodia patient in 2010 (Shan et al., 2016; Haddow et al., 2012) and is not associated with human severe neuronal disorder or microcephaly in infants in the past few years (Heang et al., 2012). The VEN/2016 strain, meanwhile, is a contemporary American strain isolated from a patient returning from Venezuela in 2016 (Zhang et al., 2016b; Li et al., 2016d). There are some amino acid variations between the CAM/2010 and VEN/2016 strains (Table S1). Since the neonatal mouse brain is relatively immature, similar to that of a second-trimester human fetus (Ornaghi et al., 2017), and ZIKV infection at this stage of pregnancy has been reported to cause microcephaly (Brasil et al., 2016; Franca et al., 2016), we adopted a neonatal mouse brain infection model to compare the effects of ZIKV CAM/2010 and VEN/2016 strains in the neonatal mouse brain (Huang et al., 2016). In this study, we found that VEN/2016 infection led to much more severe microcephaly than CAM/2010, accompanied by loss of more neurons and oligodendrocytes, and a much stronger immune response.

2. Methods and Materials

2.1. Ethics Statement

All animal work was conducted strictly according to the guidelines of the Chinese Regulations of Laboratory Animals (Ministry of Science and Technology of People's Republic of China) and Laboratory Animal-Requirements of Environment and Housing Facilities (GB 14925-2010, National Laboratory Animal Standardization Technical Committee). All of the procedures were approved by the Animal Experiment Committee of Laboratory Animal Center, Academy of Military Medical Sciences (AMMS), China (IACUC-13-2016-001).

2.2. Animals and ZIKV Inoculation

100 pfu of ZIKV (CAM/2010, an old Asian strain or VEN/2016, a South America strain) or PBS buffer (20 μL) was injected into the λ point of ICR mouse brains at postnatal 0 day and the infected brains were inspected at different time points as indicated. The mice were provided by the Laboratory Animal Center, AMMS, China. The experimental procedures on mice were performed under biosafety level 2 (BSL-2) at Beijing Institute of Microbiology and Epidemiology with Institutional Biosafety Committee approval (Li et al., 2016b).

2.3. Virus Preparation

The ZIKV stocks (both VEN/2016 and CAM/2010 strains) were from the Virus Bank of Beijing Institute of Microbiology and Epidemiology, and the isolation and characterization were performed in Cheng-Feng Qin's laboratory as described previously (Deng et al., 2016; Li et al., 2016d). The VEN/2016 of ZIKV (GenBank accession NO. KU820898) was isolated from the acute-phase serum of a patient infected with ZIKV who returned from Venezuela to China in 2016 (Li et al., 2016d). The CAM/2010 (GenBank number KU955593), the old Asian strain, was isolated from a patient in Cambodia in 2010 (Shan et al., 2016). The initial virus seeds were passaged for three rounds of serial-propagations in cultured *Aedes albopictus* C6/36 cells, purchased from the American Type Culture Collection (ATCC, NO. CRL-1660). The virus titers were measured based on the standard plaque assay on BHK-21 cells which were purchased from ATCC (NO. CCL-10), and the virus was stored at −80 °C in aliquots before used.

2.4. Immunostaining

Immunostaining was performed as described previously (Zhang et al., 2016a). Briefly, after the dissected brains were fixed in PFA (4%) and then dehydrated in sucrose (30%), these brains were frozen and sectioned into 40 μm slices using with Leica CM1950. The brain slices were first incubated in blocking buffer (10% FBS, 5% BSA, 0.3% Triton X-100, 0.01% NaN3 dissolved in PBS) at room temperature for 1 h, and then incubated in primary antibodies dissolved in blocking buffer at 4 °C for at least 8 hours, and finally incubated in fluorescence-conjugated secondary antibodies at RT for 1 h. The antibodies used for immunostaining: ZIKV anti-serum (1:1000) (Li et al., 2016a), cleaved-Caspase3 (abcam, ab2302, 1:1000), GFAP (abcam, ab7260, 1:1000), NeuN (abcam, ab104224, 1:1000), Calbindin (Millipore, ab1778, 1:200), MBP (abcam, ab7349, 1:100), CNPase (abcam, ab6319, 1:200), CD68 (abcam, ab125212, 1:500), Iba1 (abcam, ab5076, 1:500), Sox2(abcam, ab97959, 1:1000), Ki67 (abcam, ab15580, 1:1000), Olig2 (Millipore, ab9610, 1:1000).

2.5. Toluidine Blue Staining

Brain slices were stained with 0.1% toluidine blue for 30 min, dehydrated in turns by 70%, 95% and 100% ethanol (45 s, twice for each). Slices were then hyalinized by Xylene for 10 min before sealed with neutral balsam.

2.6. Alizarin Red S staining

Brain slices were incubated with 2% Alizarin Red S (pH: 4.1–4.3) at RT for 2 min, and washed in PBS for 10 min for three times.

2.7. RNA Extraction and Real-time PCR

The RNA extraction experiment was performed with PureLink® RNA Mini Kit (Thermo Fisher Scientific) according to manufactory's protocol. The Real-time PCR were performed as described previously (Schmittgen and Livak, 2008). The sequence of primers used for detecting the RNA of ZIKV was: 5′-CCGCTGCCCAACACAAG-3′ (F) and 5′-CCAC TAACGTTCTTTTGCAGACAT-3′ (R). The primer sequences used for the immune factors were shown in Table S2.

2.8. Imaging and Statistics Analysis

Confocal imaging and quantification were performed as described previously (Zhang et al., 2014). The confocal images were obtained by the Zeiss LSM700 confocal microscopy, and Leica MZ16F Stereomicroscope was used to achieve the images of Toluidine blue staining and Alizarin Red S staining. These images were analyzed with the ImageJ, Photoshop and Imaris software. For statistical analysis, *t*-test or One-Way ANOVA with Tukey's multiple comparisons test were employed to analyze the data using Prism software, and the significant difference was indicated as $^{*}P < 0.05$, $^{**}P < 0.01$, $^{***}P < 0.001$, $^{\#}P < 0.05$, $^{\#\#}P < 0.01$, $^{\#\#\#}P < 0.001$. n, number of brains analyzed. The microcephaly is defined by smaller brain sizes, enlarged lateral ventricles, and thinner cortex than controls.

3. Results

3.1. ZIKV infection by the American strain leads to more severe microcephaly than the old Asian strain

ZIKV infection at the second trimester of pregnancy in women can cause brain abnormality in children, and the neonatal mouse brain is comparable with the brain of second-trimester human fetus (Franca et al., 2016; Brasil et al., 2016). In order to investigate the effect of ZIKV infection at this stage of brain development, we injected 100 pfu

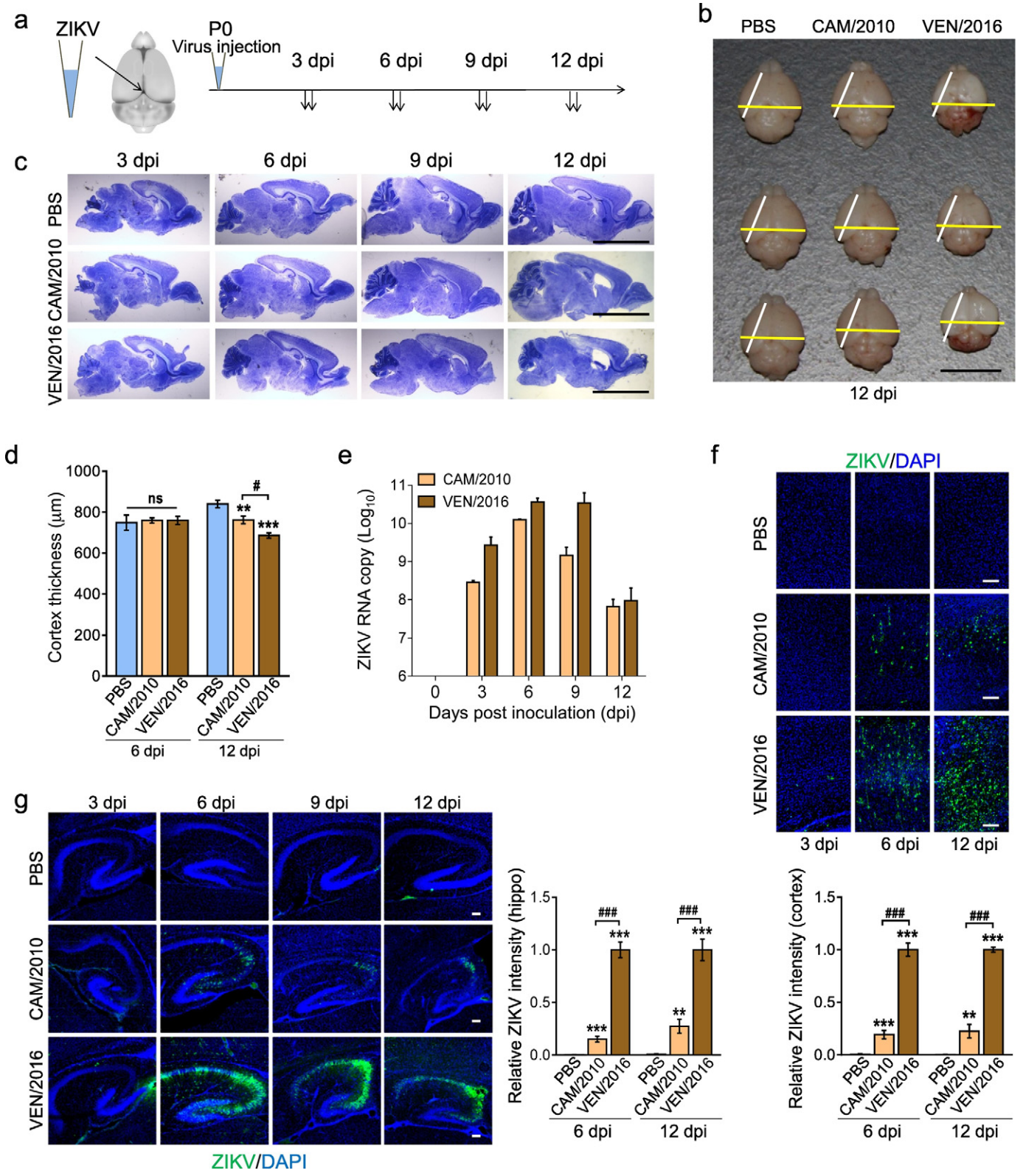

Fig. 1. Neonatal ZIKV infection of VEN/2016 leads to more severe microcephaly than CAM/2010. a. Schematic diagram showing the ZIKV infection model of neonatal mouse brains. 100 pfu of CAM/2010, VEN/2016 or PBS was injected into the λ point of mouse brain at postnatal 0 day, and brains were dissected at different time points as indicated. Without specific indication, the infected brains would mean that infection of ZIKV in the postnatal brains was performed by this procedure. b. Images of dissected ZIKV infected brains at 12 dpi. Brains infected by the VEN/2016 strain were significantly smaller than those by CAM/2010 infected. c. Images of Toluidine Blue stained sagittal sections from similar position of ZIKV infected brains at different dpi. d. Quantification analysis of thickness of infected cortical layers from the similar position of ZIKV infected brains. Data represent mean ± SEM. $^{**}P < 0.01$; $^{***}P < 0.001$; $^{\#}P < 0.05$; ns, not significant. (n = 5; one-way ANOVA). n, number of brains analyzed with two slices for each brain. e. RNA from the ZIKV infected whole brains was extracted and the viral RNA copies were determined by real-time PCR. Data represent means ± SEM from two independent experiments. f and g. Sagittal sections from ZIKV infected brains dissected at indicated dpi were stained with ZIKV antibody, and quantification of relative intensity of ZIKV staining in the CAM/2010 and VEN/2016 strain infected cortex (f) and hippocampus (g) was analyzed. Data represent mean ± SEM. $^{**}P < 0.01$; $^{***}P < 0.001$; $^{\#\#\#}P < 0.001$. (Cortex, n = 6; Hippocampus, n = 5; paired *t*-test.) Scale bars: 1 cm (b), 0.5 cm (c), 100 μm (f and g). Nuclei were stained with DAPI.

of CAM/2010 (an old Asian strain) or VEN/2016 (a contemporary American strain) or PBS buffer into the λ point of mouse brains at postnatal 0 day and inspected the brains at different days post inoculation (dpi) (Fig. 1a). At 12 dpi, the CAM/2010 infected mice had slightly smaller brain sizes, enlarged lateral ventricles, and thinner cortex than controls (Fig. 1b–d). Interestingly, the effects of VEN/2016 infection were much more dramatic, including severe microcephaly, enlarged lateral ventricles, and thinner cortex (Fig. 1b–d). In addition, VEN/2016 infection also led to more extensive calcification inside the infected brains than CAM/2010 at 12 dpi, as indicated by Alizarin Red S staining (Fig. S1a) (Rubin et al., 2016).

Infection of the brains was verified by real-time PCR and immunocytochemistry. The viral RNA copies of VEN/2016 were higher than that of CAM/2010 at 3–9 dpi, indicating that VEN/2016 could propagate more efficiently in the brain (Fig. 1e). We found that both CAM/2010 and VEN/2016 efficiently infected the cortex, hippocampus, olfactory bulb, cerebellum and striatum at 6 dpi, but not the midbrain and medulla (Fig. S1b). The ZIKV signal in the infected cortex and hippocampus regions began to emerge at 3 dpi and reached high levels at 6 dpi to 12 dpi (Fig. 1f and g). Of note, the ZIKV signal intensity and the number of infected cells in the cortex and hippocampus infected by ZIKV VEN/2016 were substantially higher than that of CAM/2010 at 6–12 dpi (Fig. 1f and g).

The thinner cortex and enlarged lateral ventricles led us to inspect and compare the cell death/apoptosis induced by the two strains in the neonatal brains. Indeed, there were many cells positive for the activated form of Caspase 3 at 9 and 12 dpi (Fig. 2a, b and data not shown). Interestingly, VEN/2016 infection induced dramatically more apoptosis than CAM/2010, consistent with its higher infection efficiency (Fig. 2a). However, little cell death was detected at 6 dpi, despite the fact that a large amount of cells were infected by VEN/2016 at this period (Fig. 2a). Most of the infected cells still had the normal morphology at 6 dpi but turned into the round shape at 9 and 12 dpi. In addition, many, although not all, of the apoptotic cells were also positive for ZIKV staining, indicating that ZIKV may induce cell death directly or maybe indirectly through the induction of immune response (Fig. 2b).

3.2. VEN/2016 Infection Leads to Loss of More Neurons in the Postnatal Brain

To define what kind of cells could be infected by ZIKV, we performed immunostaining of the brain slices at 6 dpi with antisera for ZIKV and

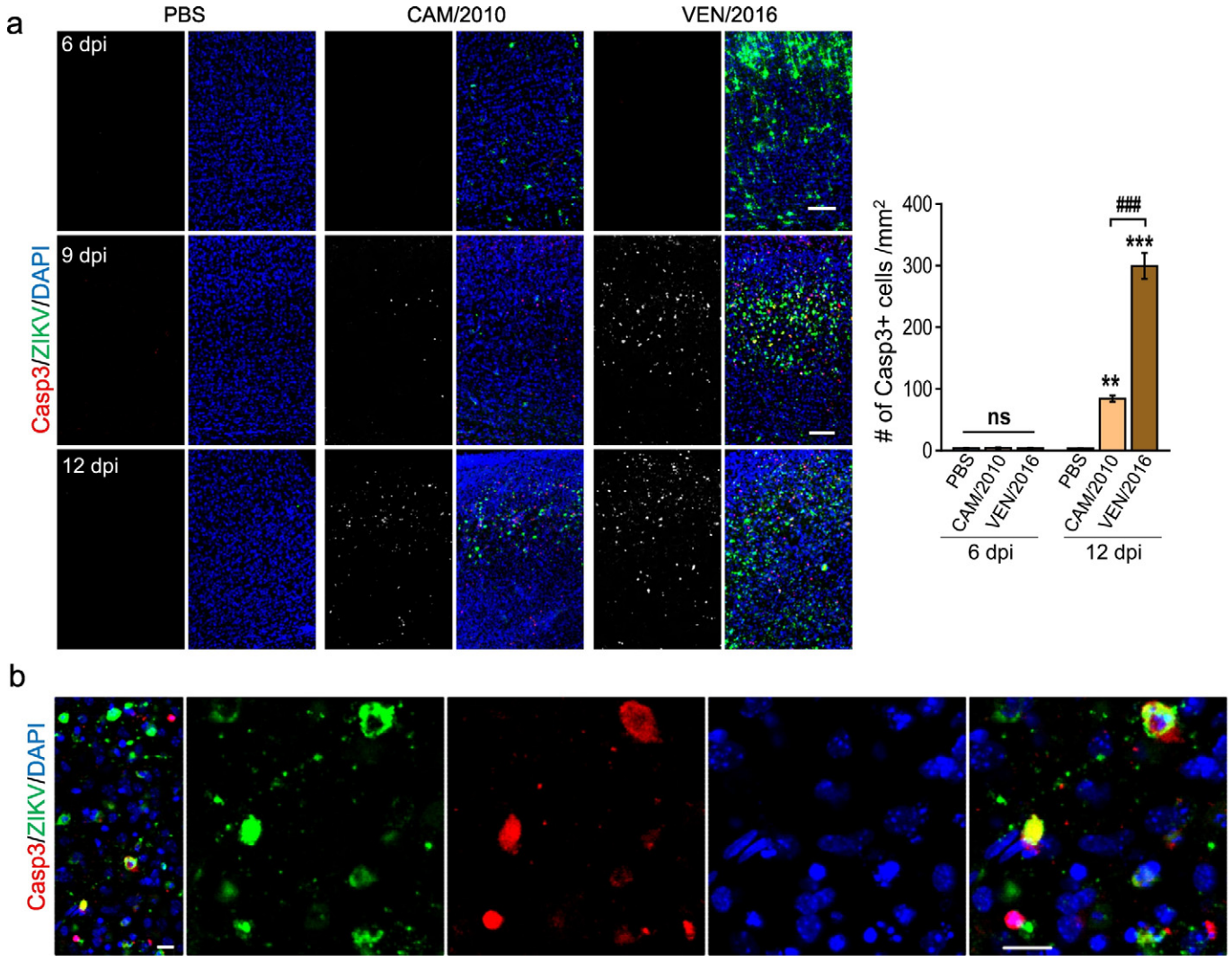

Fig. 2. Infection of VEN/2016 causes more apoptosis in the brain. a. Sagittal sections from CAM/2010 and VEN/2016 infected brains dissected at 6, 9 and 12 dpi were stained with the activated form of Caspase3 (Casp3) and ZIKV antibodies and quantification of Casp3 positive cells density in the infected regions of the six-layered cortex was analyzed. Data represent mean ± SEM. $^{**}P < 0.01$; $^{***}P < 0.001$; $^{###}P < 0.001$; ns, not significant. (n = 6; one-way ANOVA). n, number of brains analyzed. b. Confocal images of sagittal cortical sections from VEN/2016 infected brains at 9 dpi stained with Casp3 and ZIKV antibodies. Scale bars: 100 μm (a), 20 μm (b). Nuclei were stained with DAPI.

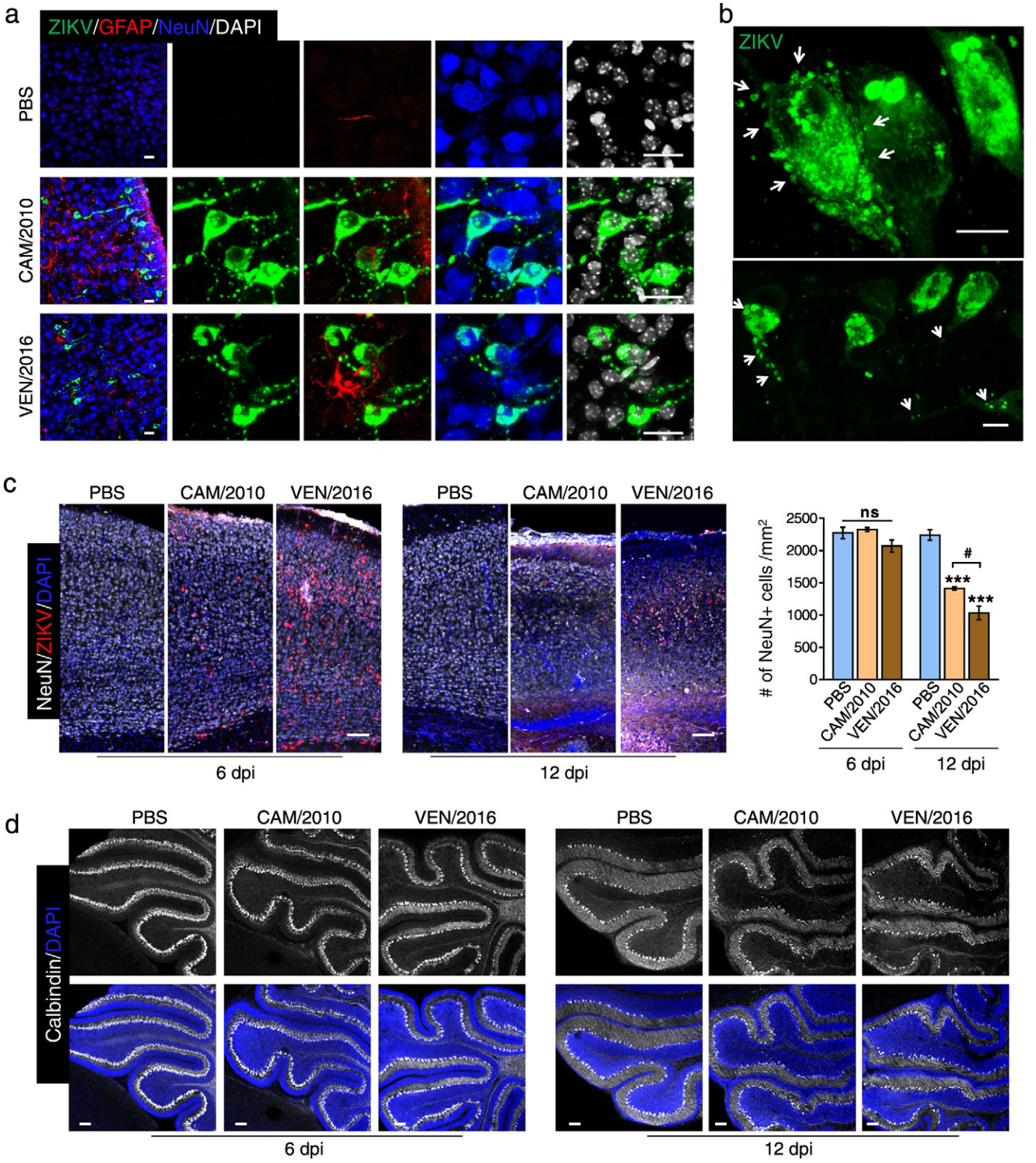

Fig. 3. VEN/2016 infection leads to loss of more neurons in different parts of the brain. a. Neurons infected by ZIKV. Confocal images of sagittal cortical sections of CAM/2010 and VEN/2016 infected brains at 6 dpi stained with NeuN, GFAP and ZIKV antibodies. b. The brains were injected with 500 pfu of VEN/2016 at postnatal 0 day and dissected at 9 dpi. Sagittal sections of infected brains were stained with ZIKV antibody and confocal images of the Purkinje's cells in the cerebellum were shown. Upper panels: Arrows indicated the viral vesicles along the cytoplasmic membrane. Lower panels: Arrows indicated the viral vesicles in the soma and in the dendrites. c. ZIKV infection leads to loss of neurons. Sagittal cortical sections of CAM/2010 and VEN/2016 infected brains dissected at 6 and 12 dpi were stained with NeuN and ZIKV antibodies. Right panel: quantification analysis of NeuN positive cells density. Data represent mean ± SEM. $^{***}P < 0.001$; $^{\#}P < 0.05$; ns, not significant. ($n = 3$; one-way ANOVA). n, number of brains analyzed. d. ZIKV infection affected Purkinje's cells. Confocal images of sagittal sections of ZIKV infected brains dissected at 6 and 12 dpi and stained with Calbindin antibody. Scale bars: 25 μm (a), 10 μm (b), 100 μm (c, d). Nuclei were stained with DAPI.

markers of different cell types, including neurons (NeuN), astrocytes (GFAP), microglial cells (Iba1) and oligodendrocytes (MBP). The majority of cells infected in the six-layered cerebral cortex were positive for NeuN, with some positive for oligodendrocytes and a few positive for other cell types (Figs. 3a, 4a, 5b and data not shown). About 94% of CAM/2010 infected cells and 93% of VEN/2016 infected cells in the six-

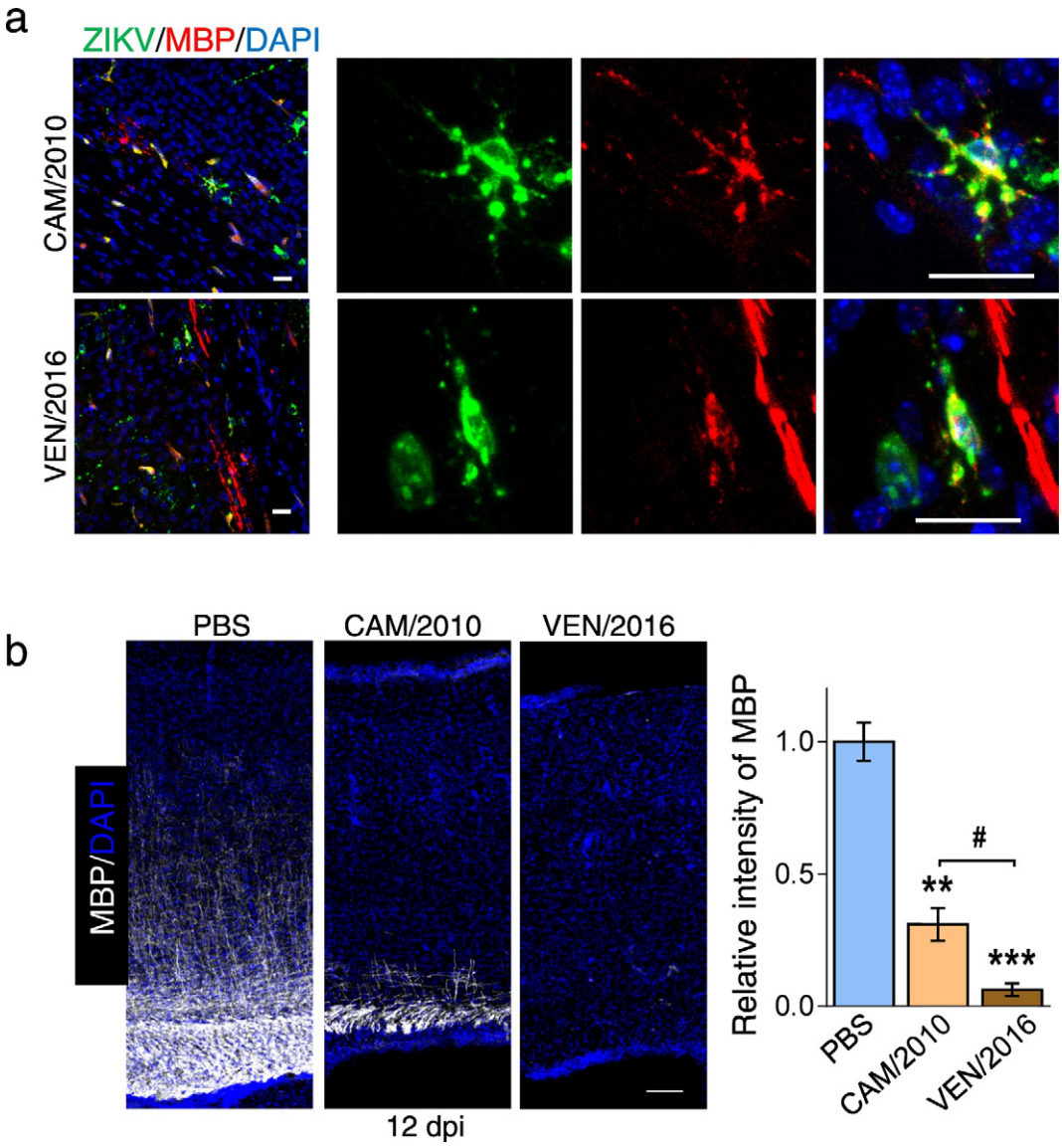

Fig. 4. ZIKV infection impairs the development of oligodendrocytes. a. ZIKV infection of oligodendrocytes. Confocal images of sagittal cortical sections of CAM/2010 and VEN/2016 infected brains at 6 dpi and stained with MBP and ZIKV antibodies. b. ZIKV infection abolished the development of oligodendrocytes. Sagittal cortical sections of CAM/2010 and VEN/2016 infected brains dissected at 6 and 12 dpi were stained with MBP antibody and quantification of the intensity of MBP staining in the infected cortex was analyzed. Data represent mean ± SEM. $^{**}P < 0.01$; $^{***}P < 0.001$; $^{\#}P < 0.05$. (n = 3; paired *t*-test). n, number of brains analyzed. Scale bars: 25 μm (a), 100 μm (b). Nuclei were stained with DAPI.

layered cerebral cortex were NeuN positive cells (Fig. S2). According to the high-resolution images of ZIKV infected Purkinje cells in cerebellum (Fig. 3b), ZIKV existed in the form of round particles in the soma and the dendrites. Some of these ZIKV enriched particles were in close contact with the cytoplasmic membrane both inside and outside of the cell, implicating that the ZIKV enriched particles were exiting from the cell through exocytosis (Fig. 3b). In accordance with the apoptosis found in the cortex, there were apparent loss of neurons ($NeuN^+$) in the ZIKV infected cortex at 12 dpi (Fig. 3c). Consistently, significantly lower neuronal density was detected in VEN/2016 infected brains than that of CAM/2010 (Fig. 3c).

Because cerebellum was also susceptible to ZIKV infection (Fig. 1 and S1), we labelled the Purkinje cells with Calbindin antibody to evaluate the effect of ZIKV on cerebellum. As shown in Fig. 3d, the soma of Purkinje cells in ZIKV infected cerebellum became misarranged, accompanied by disorganized and reduced complexity of their neuronal processes at 12 dpi.

3.3. VEN/2016 Infection Abolishes the Myelination of Oligodendrocytes

Mammalian brains are comprised of 50–90% of glial cells including oligodendrocytes, astrocytes and microglia (Zuchero and Barres, 2015; Herculano-Houzel, 2014) and 75.6% of human cerebral cortex glia cells are oligodendrocytes, which are responsible for the myelination of axons (Pelvig et al., 2008). We noticed that the thickness of the corpus callosum (CC) of ZIKV infected brains was reduced compared with that of controls at 12 dpi (Fig. 1c). Therefore, we investigated the development of oligodendrocytes at the corpus callosum and the white matter areas where oligodendrocytes are enriched. As shown in Fig. 4a and Fig. S3a, some of the MBP^+ (a marker for mature oligodendrocyte cells) and $Olig2^+$ (a marker of oligodendrocytes cells) could be infected by ZIKV in the white matter at 6 dpi. The density of $Olig2^+$ cells were significantly decreased in both CAM/2010 and VEN/2016 infected CC regions at 12 dpi (Fig. S3b). As for the myelination in ZIKV infected brains, large amount of MBP^+ cells in the white matter of control brains

could be detected at 12 dpi. In contrast, the intensity was much lower in the CAM/2010 infected brains but it was hard to detect in the VEN/2016 infected brains (Fig. 4b).

3.4. ZIKV Infection Not Only Activates Microglial Cells but also Induces Their Proliferation

Microglial cells are specialized macrophages in the brain that play important roles in inflammation and innate immune response and are capable of phagocytosis in the central nervous system (Kriegstein and Alvarez-Buylla, 2009; Zuchero and Barres, 2015). Since the activation of microglia have been suggested by previous studies (Shao et al., 2016; Vermillion et al., 2017), we compared the effect of the two ZIKV strains on the activation of microglia with Iba-1, a marker for microglial cell and CD68, a marker for phagolysosome which mainly labels the activated immune cells, including microglial cells (Ito et al., 1998; Holness and Simmons, 1993). The number of microglial cells began to increase at 3 dpi (Fig. S4a), when only a few cells were infected by ZIKV as shown in Fig. 1. At 6–12 dpi, the number of $Iba1^+$ cells and their complexity increased significantly in brains infected by either CAM/2010 or VEN/2016 (Fig. 5a and S4). Accordingly, the density of $CD68^+$ cells also increased dramatically in the infected brains at 12 dpi (Fig. 5a). Unexpectedly, it seemed that CAM/2010 infection activated more microglial cells than VEN/2016 as the cell density of $CD68^+$ cell and $Iba1^+$ cells were significantly higher in CAM/2010 infected brains (Fig. 5a), although the percentage of activated microglial cells were similar in the CAM/2010 and VEN/2016 infected cerebral cortex (88% and 91%, respectively) (Fig. S5a). As shown in the enlarged images in Fig. 5b, microglial cells were found to locate around or be in contact with the infected cells at 6 dpi. Interestingly, some infected neurons were detected to be engulfed by microglial cells at 12 dpi. (Fig. 5b)

The substantial increase of microglial cell number indicated that ZIKV might not only activate microglia, but also induce their proliferation. Indeed, as shown in Fig. 5c and d, through immunostaining of the cortex with antibodies for Sox2 (a marker for stem or progenitor cells) and Ki67 (a marker for proliferating cells), we found that some of the $Iba1^+$ cells were also positive for Sox2 or Ki67 in both CAM/2010 and VEN/2016 infected cortex, implying that ZIKV might induce the proliferation of microglial cells.

3.5. VEN/2016 Strain Infection Induces More Severe Immune Response

ZIKV has been reported recently to induce strong immune response in both cultured NPC and in the brain (Tang et al., 2016; Li et al., 2016b; Li et al., 2016c; Wu et al., 2016; Rasmussen et al., 2016; Tappe et al., 2016). We went on to inspect the effect of the two different ZIKV strains on immune response in the brain. Total RNA were purified from the whole infected brain and subjected to real-time PCR for the analysis of the expression of different immune response factors. We found that both CAM/2010 and VEN/2016 strains could induce the expression of many immune response factors, such as TNF-α, IFN-α, IL-10, IL-2, MCP1 (Fig. 6). Nevertheless, the levels of these factors induced by VEN/2016 were significantly or substantially higher than that by CAM/2010 at 6 dpi or 12 dpi, indicating that VEN/2016 tends to induce stronger immune response than CAM/2010.

4. Discussion

In this study, we inject a very small amount of ZIKV (100 pfu) into the λ point of the neonatal mouse brain to generate a ZIKV infection model with straight-forward manipulation and reproducibility. Both CAM/2010 and VEN/2016 ZIKV strains can efficiently infect the mouse brain and propagate in the postnatal brains for >12 days before their elimination. ZIKV infects different parts of the brain with high efficiency. This indicates that ZIKV injected into the λ point of the brain can spread from cell-to-cell and/or disperse through the cerebrospinal fluid to nearly the whole brain. Our detection of the ZIKV enriched particles in the soma and dendrite raises the possibility of virus transmission along the dendrite or axon from one neuron to another one located at far distance to increase the efficiency of infection.

We observed the dynamic process of ZIKV infection in the neonatal mouse brain. After injection of ZIKV in the brain at postnatal 0 day, the viral RNA copies of ZIKV began to amplify and only a few cells expressed ZIKV antigen in their cytoplasm at 3 dpi, but the microglia were activated likely due to early immune response. At 6 dpi, a large amount of cells, including neurons and oligodendrocytes, were infected by ZIKV and the viral RNA copies in the infected brains reached the climax. However, at this time point, ZIKV infection did not induce very significant cell apoptosis and the morphology of neurons remained largely normal, while the activated microglia in contact with infected cells were detected. At 9 dpi, cell apoptosis became evident and the cells started to turn into a round shape. At 12 dpi, the VEN/2016 infected brains showed significant microcephaly, accompanied with a much thinner cortex, calcification, extensive apoptosis and dramatic loss of neurons and oligodendrocytes. However, the viral RNA copies of ZIKV dropped significantly at this time point, and we observed that the infected cells could be engulfed by microglia, indicating that ZIKV could be eliminated at the expense of getting rid of those infected cells.

Both ZIKV strains, CAM/2010 (an old Asian strain) and VEN/2016 (an American strain), can infect the neonatal mouse brain and cause some similar phenotypes, such as cell death, defect in oligodendrocyte development, activation of microglial cells, and induction of immune response. However, there are significant differences between them. Compared with CAM/2010, VEN/2016 infects the brains more efficiently and leads to much more severe microcephaly. In addition, VEN/2016 strain infection leads to stronger immune response, more severe calcification, more neuronal death and abolished oligodendrocyte development, but less activation of microglial cells. Thus, the more severe damage caused by VEN/2016 might explain why the American ZIKV strain can lead to severe microcephaly in human fetus or infant in South America since 2015 (Garcez et al., 2016; Miner et al., 2016; Parra et al., 2016; Rubin et al., 2016), while the old Asian strain was not associated with such severe disorders (Heang et al., 2012). It is interesting to note that the only effect induced by VEN/2016, which is not as significant as CAM/2010, is the activation of microglial cells in the late stage of infection (at 12 dpi). Since ZIKV infected cells could be engulfed and digested by the activated microglial cells, it might be possible that this may account for, in part, why VEN/2016 propagates much faster in the brain than CAM/2010. On the other hand, VEN/2016 might infect more cells to make microglial cells overloaded and get cleaned up.

Although some cells undergoing apoptosis in the ZIKV infected brains were positive for ZIKV staining, many of them were not infected. Therefore, it is hard to conclude that the ZIKV killed the infected cells directly. Notably, as is shown in Fig. 2b, the cells were filled with viral vesicles, and the vesicles were even "overflowing" from the cells, however, the morphology of the cells were largely normal. This raises the possibility that apoptosis of cells was caused by the immune response induced by ZIKV infection. Indeed, VEN/2016 which induced more severe immune response than CAM/2010, led to extensive loss of cells and much smaller brains.

We observed that some oligodendrocytes were infected by ZIKV, and that the density of $Olig2^+$ cells were reduced similarly in CAM/2010 and VEN/2016 (39% and 40% respectively) in ZIKV infected CC region, compared with loss of 60% and 94% MBP expression. This indicated that ZIKV infection could lead to loss of oligodendrocytes, which would partially contribute to the reduction of MBP expression. Despite the loss of oligodendrocytes, the more dramatic decrease of MBP intensity in VEN/2016 infected brains than CAM/2010 was likely resulting from more dramatic loss of neurons and subsequently depletion of myelination in VEN/2016 infected brains. Another very likely possibility is that the much stronger immune response induced by VEN/2016

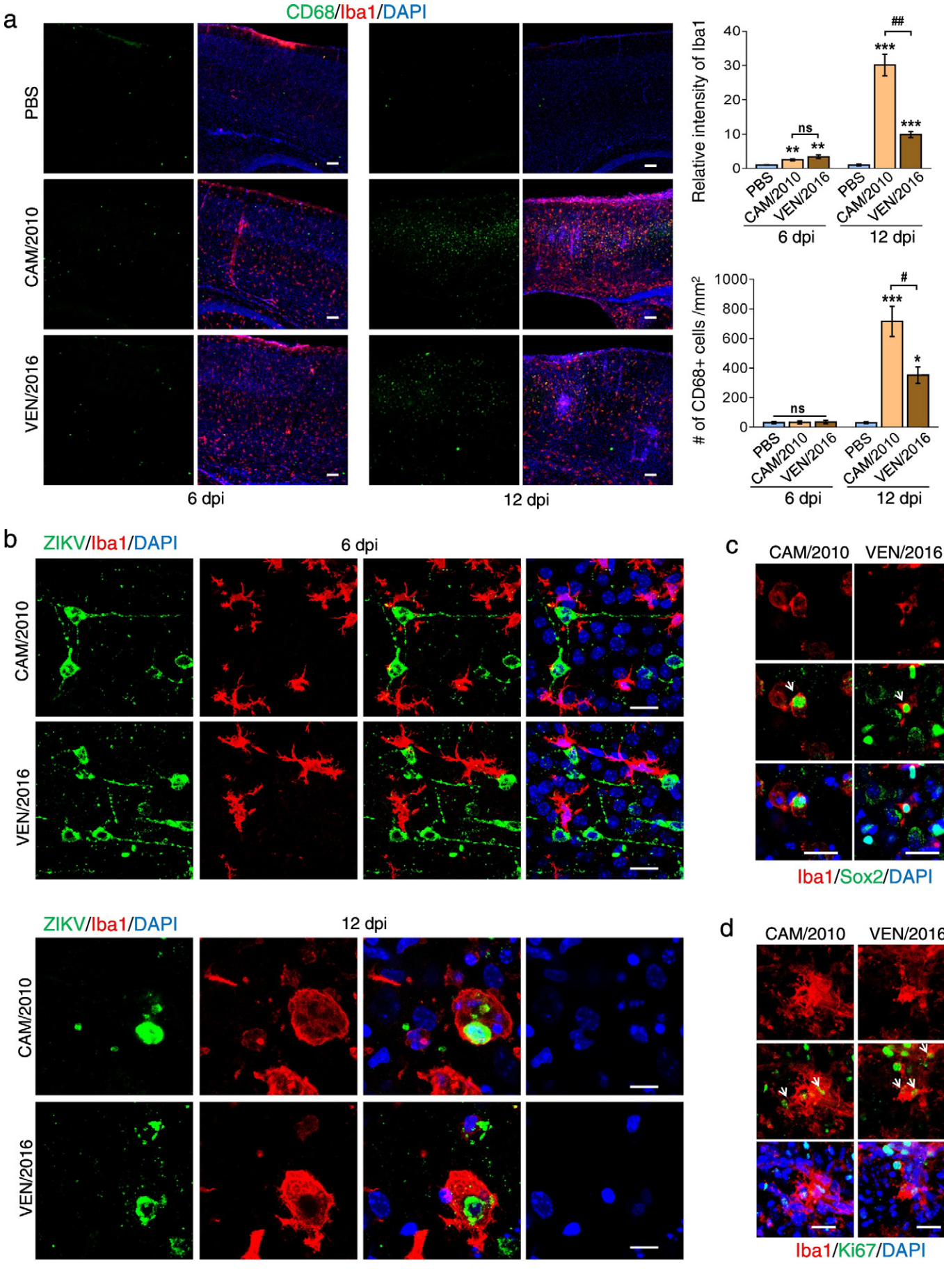
a
CD68/Iba1/DAPI
PBS
CAM/2010
VEN/2016
6 dpi
12 dpi
Relative intensity of Iba1
40
30
20
10
0
ns
**
**
***
***
##
PBS
CAM/2010
VEN/2016
6 dpi
12 dpi
# of CD68+ cells /mm2
1000
800
600
400
200
0
ns
***
*
#
b
ZIKV/Iba1/DAPI
6 dpi
CAM/2010
VEN/2016
ZIKV/Iba1/DAPI
12 dpi
CAM/2010
VEN/2016
c
CAM/2010
VEN/2016
Iba1/Sox2/DAPI
d
CAM/2010
VEN/2016
Iba1/Ki67/DAPI

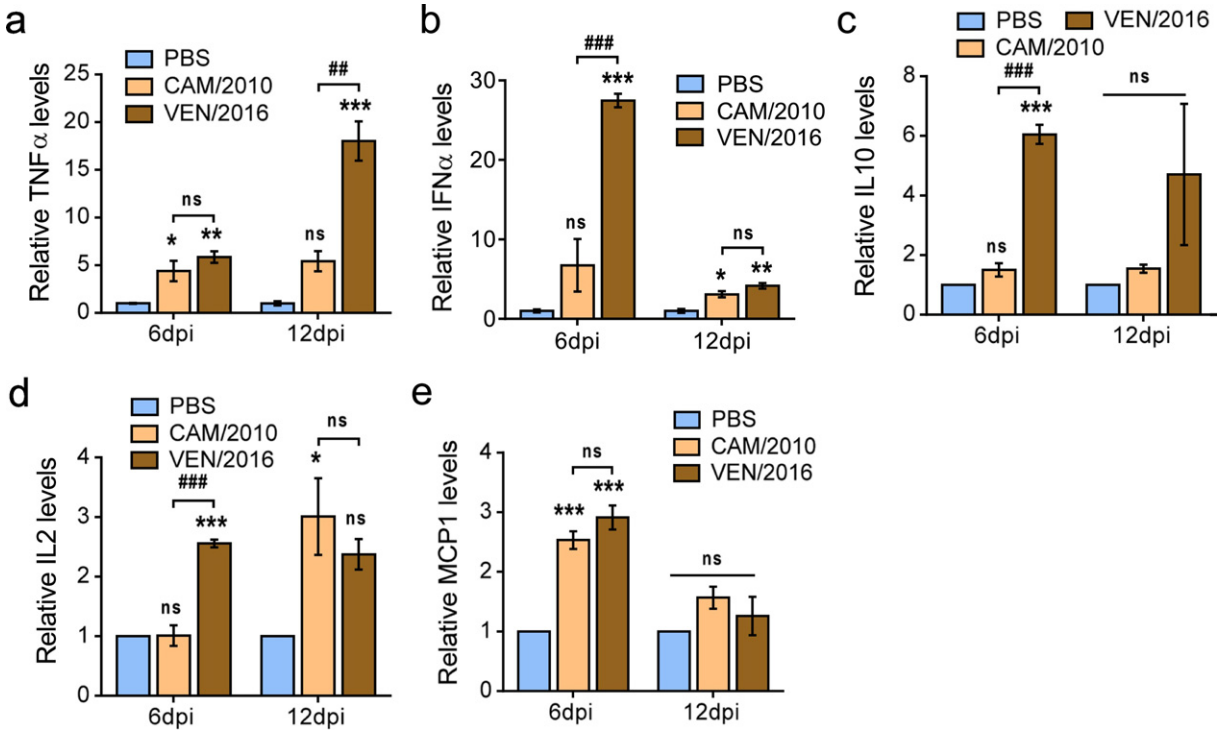

Fig. 6. Infection of VEN/2016 induces stronger immune response than CAM/2010. a–e. RNA of the whole brains infected by CAM/2010 and VEN/2016 was extracted at 6 and 12 dpi, and the expression levels of indicated cytokines were determined by real-time PCR. Data represent mean ± SEM. *P < 0.05; **P < 0.01; ***P < 0.001; ##P < 0.01; ###P < 0.001; ns, not significant. (n = 3; one-way ANOVA).

which may inhibit the differentiation of oligodendrocyte progenitor cells to mature oligodendrocytes, or the cell death of MBP^+ cells.

Minor microcephaly and fetal brain lesions, including cerebral white matter hypoplasia, periventricular white matter gliosis, and axonal and ependymal injury, after subcutaneous inoculation of Zika virus (CAM/2010) in a pregnant nonhuman primate has been reported recently (Adams Waldorf et al., 2016). This is in agreement with our finding that CAM/2010 infection can result in damages in the brain. It will be intriguing to inspect, in the future, whether contemporary American Zika will cause much more severe damages in the nonhuman primate fetal brain. It is worth notice that 5×10^7 PFU has been used for the nonhuman primate study which is dramatically higher than that we used in mouse (100 PFU) even considering the difference between body weights. Subcutaneous inoculation of very large amount of Zika virus would lead to intensive immune response in the pregnant mother which will affect the brain development indirectly. Therefore, much smaller amount of ZIKV would be recommended for future study.

Much higher neurovirulence of several contemporary American Zika strains has been reported during the revision of this manuscript (Yuan et al., 2017). In addition, VEN/2016 infection of the E13.5 brain (comparable with the first-trimester human fetus brain) also results in more extensive damages than CAM/2010, including smaller brain, dysregulation of the proliferation and differentiation of the neuronal progenitor cell, and cell death. Together with the results in this study, we can conclude that the contemporary American Zika strain has more detrimental effects than the ancestral Asian strain infection in both early and middle stages of brain development, and would explain why the infection of pregnant women with the contemporary American Zika strain, but not the ancestral African or Asian strains, has been reported to result in microcephaly.

It is very important to define what happened to ZIKV during the last several years which enabled the American strain to cause severe microcephaly in mouse and human. The genome of ZIKV is a single-stranded RNA, which encodes the structural proteins capsid (C), pre-membrane protein (prM), envelope (E) and some non-structural proteins (Kuno and Chang, 2007; Wang et al., 2016; Zhang et al., 2012). There are some differences or mutations between the genomes of CAM/2010 and VEN/2016 strains, some of which may account for the difference between CAM/2010 and VEN/2016 in infection efficiency and neurovirulence. Interestingly, a single mutation (S139N) in the prM protein of CAM/2010 Zika virus has been found to contribute to more severe fetal microcephaly, and this mutation of ZIKV arose around the outbreak in French Polynesia (2013) and was stably maintained during subsequent spread to the Americas, suggesting that this functional adaption makes ZIKV more neurovirulent to cause the microcephaly in infected human fetus (Yuan et al., 2017). However, we need to screen for more mutations to investigate whether other mutations, in addition to the S139N mutation, play important roles in the enhanced neurovirulence and detrimental effects on brain development. This will certainly help to improve our understanding of the pathogenesis of American ZIKV strain.

In summary, we adopted the postnatal mouse brain ZIKV infection model by injecting the virus into the neonatal brains and investigated the dynamic effects of ZIKV infection in the postnatal brains. We confirmed that ZIKV could replicate efficiently to infect most parts of the brains and cause damage to different types of cells. Importantly, VEN/

Fig. 5. ZIKV infection in the postnatal brains leads to the activation of microglial cells. a. Confocal images of sagittal cortical sections of CAM/2010 and VEN/2016 infected brains dissected at 6 and 12 dpi and stained with Iba1 and CD68 antibodies. Right panels: quantification analysis of intensity of Iba1 staining (upper panel) and CD68 positive cell density (lower panel) in the infected cortex at 6 and 12 dpi. Data represent mean ± SEM. *P < 0.05; **P < 0.01; ***P < 0.001; #P < 0.05; ##P < 0.01; ns, not significant. (n = 3; Iba1: paired t-test; CD68: one-way ANOVA). n, number of brains analyzed. b. ZIKV infected cells engulfed microglial cells. Sagittal cortical sections of infected brains dissected at 6 and 12 dpi were stained with Iba1 and ZIKV antibodies. c-d. Sagittal cortical sections of CAM/2010 and VEN/2016 infected brains dissected at 12 dpi were stained with Sox2 (c) or Ki67 (d) and Iba1 antibodies. Scale bars: 100 μm (a), 10 μm (b), 20 μm (c, d). Nuclei were stained with DAPI.

2016 infection led to more cell death and more severe microcephaly than CAM2010. Therefore, the determination of different ZIKV strains would be helpful for doctors to propose the proper treatment of pregnant women in the future. In addition, our postnatal mouse infection model would provide a platform for the screening of anti-ZIKV drugs or vaccines.

Acknowledgements

We would like to thank Dr. Weixiang Guo and Dr. Xia Jin for critical reagents, information and helpful discussion.

Funding Sources

This work was supported by the National Natural Science Foundation (NSFC) of China (31430037/31730108), Innovation Program of the Chinese Academy of Sciences (QYZDJ-SSWSMC007), Shanghai brain-intelligence project from STCSM (16JC1420500), Beijing brain project (Z161100002616004) to Z.XU, and the NSFC (81522025, 81661130162, 81661148054, 81621005), the National Key Research and Development Project of China (No.2016YFD0500304), the National Science and Technology Major Project of China (No.2017ZX09101005 and No.2017ZX10304402), and the Newton Advanced Fellowship from the UK Academy of Medical Sciences (NAF003/1003) to C.-F.Q. The funders had no role in study design, data collection and analysis, decision to publish, or preparation of the manuscript.

Conflicts of Interest

None.

Author Contributions

F.Z., H.W. and Q.W. drafted the manuscript and performed the most part of the experiments; Z.L., L.Y. and X.H. prepared the ZIKV, performed the inoculation of ZIKV and analyzed the data. G.L. and Q.Y. performed the inoculation of ZIKV. H.Y., L.S. and Y.D. analyzed some part of data. C.Q. and Z.X. figured out the conception and designed the study. All authors revised the manuscript and approved the final version of manuscript.

Appendix A. Supplementary Data

Supplementary data to this article can be found online at https://doi.org/10.1016/j.ebiom.2017.10.019.

References

Adams Waldorf, K.M., Stencel-Baerenwald, J.E., Kapur, R.P., Studholme, C., Boldenow, E., Vornhagen, J., Baldessari, A., Dighe, M.K., Thiel, J., Merillat, S., Armistead, B., Tisoncik-Go, J., Green, R.R., Davis, M.A., Dewey, E.C., Fairgrieve, M.R., Gatenby, J.C., Richards, T., Garden, G.A., Diamond, M.S., Juul, S.E., Grant, R.F., Kuller, L., Shaw, D.W., Ogle, J., Gough, G.M., Lee, W., English, C., Hevner, R.F., Dobyns, W.B., Gale Jr., M., Rajagopal, L., 2016. Fetal brain lesions after subcutaneous inoculation of Zika virus in a pregnant nonhuman primate. Nat. Med. 22, 1256–1259.

Brasil, P., Pereira Jr., J.P., Moreira, M.E., Ribeiro Nogueira, R.M., Damasceno, L., Wakimoto, M., Rabello, R.S., Valderramos, S.G., Halai, U.A., Salles, T.S., Zin, A.A., Horovitz, D., Daltro, P., Boechat, M., Raja Gabaglia, C., Carvalho de Sequeira, P., Pilotto, J.H., Medialdea-Carrera, R., Cotrim da Cunha, D., Abreu de Carvalho, L.M., Pone, M., Machado Siqueira, A., Calvet, G.A., Rodrigues Baiao, A.E., Neves, E.S., Nassar de Carvalho, P.R., Hasue, R.H., Marschik, P.B., Einspieler, C., Janzen, C., Cherry, J.D., Bispo De Filippis, A.M., Nielsen-Saines, K., 2016. Zika virus infection in pregnant women in Rio de Janeiro. N. Engl. J. Med. 375, 2321–2334.

Cao-Lormeau, V.M., Roche, C., Teissier, A., Robin, E., Berry, A.L., Mallet, H.P., Sall, A.A., Musso, D., 2014. Zika virus, French polynesia, South pacific, 2013. Emerg. Infect. Dis. 20, 1085–1086.

Deng, Y.Q., Zhao, H., Li, X.F., Zhang, N.N., Liu, Z.Y., Jiang, T., Gu, D.Y., Shi, L., He, J.A., Wang, H.J., Sun, Z.Z., Ye, Q., Xie, D.Y., Cao, W.C., Qin, C.F., 2016. Isolation, identification and genomic characterization of the Asian lineage Zika virus imported to China. Sci. China Life Sci. 59, 428–430.

Duffy, M.R., Chen, T.H., Hancock, W.T., Powers, A.M., Kool, J.L., Lanciotti, R.S., Pretrick, M., Marfel, M., Holzbauer, S., Dubray, C., Guillaumot, L., Griggs, A., Bel, M., Lambert, A.J., Laven, J., Kosoy, O., Panella, A., Biggerstaff, B.J., Fischer, M., Hayes, E.B., 2009. Zika virus outbreak on Yap Island, Federated States of Micronesia. N. Engl. J. Med. 360, 2536–2543.

Franca, G.V., Schuler-Faccini, L., Oliveira, W.K., Henriques, C.M., Carmo, E.H., Pedi, V.D., Nunes, M.L., Castro, M.C., Serruya, S., Silveira, M.F., Barros, F.C., Victora, C.G., 2016. Congenital Zika virus syndrome in Brazil: a case series of the first 1501 livebirths with complete investigation. Lancet 388, 891–897.

Garcez, P.P., Loiola, E.C., Madeiro Da Costa, R., Higa, L.M., Trindade, P., Delvecchio, R., Nascimento, J.M., Brindeiro, R., Tanuri, A., Rehen, S.K., 2016. Zika virus impairs growth in human neurospheres and brain organoids. Science 352, 816–818.

Haddow, A.D., Schuh, A.J., Yasuda, C.Y., Kasper, M.R., Heang, V., Huy, R., Guzman, H., Tesh, R.B., Weaver, S.C., 2012. Genetic characterization of Zika virus strains: geographic expansion of the Asian lineage. PLoS Negl. Trop. Dis. 6, e1477.

Hayes, E.B., 2009. Zika virus outside Africa. Emerg. Infect. Dis. 15, 1347–1350.

Heang, V., Yasuda, C.Y., Sovann, L., Haddow, A.D., Travassos Da Rosa, A.P., Tesh, R.B., Kasper, M.R., 2012. Zika virus infection, Cambodia, 2010. Emerg. Infect. Dis. 18, 349–351.

Herculano-Houzel, S., 2014. The glia/neuron ratio: how it varies uniformly across brain structures and species and what that means for brain physiology and evolution. Glia 62, 1377–1391.

Holness, C.L., Simmons, D.L., 1993. Molecular cloning of CD68, a human macrophage marker related to lysosomal glycoproteins. Blood 81, 1607–1613.

Huang, W.C., Abraham, R., Shim, B.S., Choe, H., Page, D.T., 2016. Zika virus infection during the period of maximal brain growth causes microcephaly and corticospinal neuron apoptosis in wild type mice. Sci Rep 6, 34793.

Ito, D., Imai, Y., Ohsawa, K., Nakajima, K., Fukuuchi, Y., Kohsaka, S., 1998. Microglia-specific localisation of a novel calcium binding protein, Iba1. Brain Res. Mol. Brain Res. 57, 1–9.

Kriegstein, A., Alvarez-Buylla, A., 2009. The glial nature of embryonic and adult neural stem cells. Annu. Rev. Neurosci. 32, 149–184.

Kuno, G., Chang, G.J., 2007. Full-length sequencing and genomic characterization of Bagaza, Kedougou, and Zika viruses. Arch. Virol. 152, 687–696.

Li, C., Xu, D., Ye, Q., Hong, S., Jiang, Y., Liu, X., Zhang, N., Shi, L., Qin, C.F., Xu, Z., 2016a. Zika virus disrupts neural progenitor development and leads to microcephaly in mice. Cell Stem Cell 19, 120–126.

Li, C., Xu, D., Ye, Q., Hong, S., Jiang, Y., Liu, X., Zhang, N., Shi, L., Qin, C.F., Xu, Z., 2016b. Zika virus disrupts neural progenitor development and leads to microcephaly in mice. Cell Stem Cell 19, 672.

Li, H., Saucedo-Cuevas, L., Regla-Nava, J.A., Chai, G., Sheets, N., Tang, W., Terskikh, A.V., Shresta, S., Gleeson, J.G., 2016c. Zika virus infects neural progenitors in the adult mouse brain and alters proliferation. Cell Stem Cell 19, 593–598.

Li, X.F., Dong, H.L., Huang, X.Y., Qiu, Y.F., Wang, H.J., Deng, Y.Q., Zhang, N.N., Ye, Q., Zhao, H., Liu, Z.Y., Fan, H., An, X.P., Sun, S.H., Gao, B., Fa, Y.Z., Tong, Y.G., Zhang, F.C., Gao, G.F., Cao, W.C., Shi, P.Y., Qin, C.F., 2016d. Characterization of a 2016 clinical isolate of Zika virus in non-human primates. EBioMedicine 12, 170–177.

Miner, J.J., Cao, B., Govero, J., Smith, A.M., Fernandez, E., Cabrera, O.H., Garber, C., Noll, M., Klein, R.S., Noguchi, K.K., Mysorekar, I.U., Diamond, M.S., 2016. Zika virus infection during pregnancy in mice causes placental damage and fetal demise. Cell 165, 1081–1091.

Mlakar, J., Korva, M., Tul, N., Popovic, M., Poljsak-Prijatelj, M., Mraz, J., Kolenc, M., Resman Rus, K., Vesnaver Vipotnik, T., Fabjan Vodusek, V., Vizjak, A., Pizem, J., Petrovec, M., Avsic Zupanc, T., 2016. Zika virus associated with microcephaly. N. Engl. J. Med. 374, 951–958.

Ornaghi, S., Hsieh, L.S., Bordey, A., Vergani, P., Paidas, M.J., Van Den Pol, A.N., 2017. Valnoctamide inhibits cytomegalovirus infection in developing brain and attenuates neurobehavioral dysfunctions and brain abnormalities. J. Neurosci. 37, 6877–6893.

Parra, B., Lizarazo, J., Jimenez-Arango, J.A., Zea-Vera, A.F., Gonzalez-Manrique, G., Vargas, J., Angarita, J.A., Zuniga, G., Lopez-Gonzalez, R., Beltran, C.L., Rizcala, K.H., Morales, M.T., Pacheco, O., Ospina, M.L., Kumar, A., Cornblath, D.R., Munoz, L.S., Osorio, L., Barreras, P., Pardo, C.A., 2016. Guillain-Barre syndrome associated with Zika virus infection in Colombia. N. Engl. J. Med. 375, 1513–1523.

Pelvig, D.P., Pakkenberg, H., Stark, A.K., Pakkenberg, B., 2008. Neocortical glial cell numbers in human brains. Neurobiol. Aging 29, 1754–1762.

Rasmussen, S.A., Jamieson, D.J., Honein, M.A., Petersen, L.R., 2016. Zika virus and birth defects—reviewing the evidence for causality. N. Engl. J. Med. 374, 1981–1987.

Rubin, E.J., Greene, M.F., Baden, L.R., 2016. Zika virus and microcephaly. N. Engl. J. Med. 374, 984–985.

Schmittgen, T.D., Livak, K.J., 2008. Analyzing real-time PCR data by the comparative C(T) method. Nat. Protoc. 3, 1101–1108.

Shan, C., Xie, X., Muruato, A.E., Rossi, S.L., Roundy, C.M., Azar, S.R., Yang, Y., Tesh, R.B., Bourne, N., Barrett, A.D., Vasilakis, N., Weaver, S.C., Shi, P.Y., 2016. An infectious cDNA clone of Zika virus to study viral virulence, mosquito transmission, and antiviral inhibitors. Cell Host Microbe 19, 891–900.

Shao, Q., Herrlinger, S., Yang, S.L., Lai, F., Moore, J.M., Brindley, M.A., Chen, J.F., 2016. Zika virus infection disrupts neurovascular development and results in postnatal microcephaly with brain damage. Development 143, 4127–4136.

Tang, H., Hammack, C., Ogden, S.C., Wen, Z., Qian, X., Li, Y., Yao, B., Shin, J., Zhang, F., Lee, E.M., Christian, K.M., Didier, R.A., Jin, P., Song, H., Ming, G.L., 2016. Zika virus infects human cortical neural progenitors and attenuates their growth. Cell Stem Cell 18, 587–590.

Tappe, D., Perez-Giron, J.V., Zammarchi, L., Rissland, J., Ferreira, D.F., Jaenisch, T., Gomez-Medina, S., Gunther, S., Bartoloni, A., Munoz-Fontela, C., Schmidt-Chanasit, J., 2016. Cytokine kinetics of Zika virus-infected patients from acute to reconvalescent phase. Med. Microbiol. Immunol. 205, 269–273.

Vermillion, M.S., Lei, J., Shabi, Y., Baxter, V.K., Crilly, N.P., Mclane, M., Griffin, D.E., Pekosz, A., Klein, S.L., Burd, I., 2017. Intrauterine Zika virus infection of pregnant immunocompetent mice models transplacental transmission and adverse perinatal outcomes. Nat. Commun. 8, 14575.

Wang, L., Valderramos, S.G., Wu, A., Ouyang, S., Li, C., Brasil, P., Bonaldo, M., Coates, T., Nielsen-Saines, K., Jiang, T., Aliyari, R., Cheng, G., 2016. From mosquitos to humans: genetic evolution of Zika virus. Cell Host Microbe 19, 561–565.

Wu, K.Y., Zuo, G.L., Li, X.F., Ye, Q., Deng, Y.Q., Huang, X.Y., Cao, W.C., Qin, C.F., Luo, Z.G., 2016. Vertical transmission of Zika virus targeting the radial glial cells affects cortex development of offspring mice. Cell Res. 26, 645–654.

Yuan, L., Huang, X.Y., Liu, Z.Y., Zhang, F., Zhu, X.L., Yu, J.Y., Ji, X., Xu, Y.P., Li, G., Li, C., Wang, H.J., Deng, Y.Q., Wu, M., Cheng, M.L., Ye, Q., Xie, D.Y., Li, X.F., Wang, X., Shi, W., Hu, B., Shi, P.Y., Xu, Z., Qin, C.F., 2017. A single mutation in the prM protein of Zika virus contributes to fetal microcephaly. Science https://doi.org/10.1126/science.aam7120.

Zhang, Q., Hunke, C., Yau, Y.H., Seow, V., Lee, S., Tanner, L.B., Guan, X.L., Wenk, M.R., Fibriansah, G., Chew, P.L., Kukkaro, P., Biukovic, G., Shi, P.Y., Shochat, S.G., Gruber, G., Lok, S.M., 2012. The stem region of premembrane protein plays an important role in the virus surface protein rearrangement during dengue maturation. J. Biol. Chem. 287, 40525–40534.

Zhang, F., Xu, D., Yuan, L., Sun, Y., Xu, Z., 2014. Epigenetic regulation of Atrophin1 by lysine-specific demethylase 1 is required for cortical progenitor maintenance. Nat. Commun. 5, 5815.

Zhang, F., Yu, J., Yang, T., Xu, D., Chi, Z., Xia, Y., Xu, Z., 2016a. A novel c-Jun N-terminal kinase (JNK) signaling complex involved in neuronal migration during brain development. J. Biol. Chem. 291, 11466–11475.

Zhang, F.C., Li, X.F., Deng, Y.Q., Tong, Y.G., Qin, C.F., 2016b. Excretion of infectious Zika virus in urine. Lancet Infect. Dis. 16, 641–642.

Zuchero, J.B., Barres, B.A., 2015. Glia in mammalian development and disease. Development 142, 3805–3809.